

Upgrading Engine Test Cells for Improved Troubleshooting and Diagnostics

Michael J. Roemer
Rolf F. Orsagh
Gregory J. Kacprzynski
Impact Technologies, LLC
125 Tech Park Drive
Rochester, New York 14623

James Scheid
Sytronics, Inc
4433 Dayton-Xenia Rd.
Dayton, OH 45432

Wing Cmdr. Richard Friend
William Sotomayer
AFRL/PRTC
1950 Fifth Street, Bldg. 18
Wright-Patterson AFB
Dayton, Ohio 45433

Abstract

Upgrading military engine test cells with advanced diagnostic and troubleshooting capabilities will play a critical role in increasing aircraft availability and test cell effectiveness while simultaneously reducing engine operating and maintenance costs. Sophisticated performance and mechanical anomaly detection and fault classification algorithms utilizing thermodynamic, statistical, and empirical engine models are now being implemented as part of a United States Air Force Advanced Test Cell Upgrade Initiative. Under this program, a comprehensive set of real-time and post-test diagnostic software modules, including sensor validation algorithms, performance fault classification techniques and vibration feature analysis are being developed. An automated troubleshooting guide is also being implemented to streamline the troubleshooting process for both inexperienced and experienced technicians. This artificial intelligence based tool enhances the conventional troubleshooting tree architecture by incorporating probability of occurrence statistics to optimize the troubleshooting path. This paper describes the development and implementation of the F404 engine test cell upgrade at the Jacksonville Naval Air Station.

1. INTRODUCTION

A great opportunity exists within the USAF and US Navy to provide an upgraded gas turbine engine test cell diagnostic capability that will help reduce engine troubleshooting and turn-around times, while increasing safety and engine availability. In the long term, the goal is to make gas turbine engines more reliable and maintainable through the use of improved test cell diagnostic technologies. This goal can be achieved primarily through the integration, for the first time, of established trending/statistical technologies into advanced fault diagnostic systems currently being developed. To enable this, test cell fault detection and isolation capabilities will need to utilize all of the relevant engine and test cell facility information in the most efficient manner possible for improving the confidence and accuracy of troubleshooting or diagnostic approaches.

Some of the benefits of implementing advanced engine

test cell diagnostics with technologies that have been developed and demonstrated to-date include the following (Gladney, 1998 and Roemer, et al. 2001):

1. Ability to obtain increased confidence levels for a wider range of detectable faults during ground test controlled operation. Statistical fault classifiers give consistent levels of diagnosis confidence and severity for all potential faults, while retaining the ability to diagnose unexpected anomalies never seen before.
2. The utilization of proven Gas Path Analysis models provides robust fault classification with respect to measurement uncertainties, random fluctuations, and transient test cell conditions.
3. Provide detailed pre and post test analysis of all measured parameters with respect to themselves (auto correlation) and all other parameters (cross correlation) for detecting various sensor problems. This provides a necessary condition check for sensor validation procedures.
4. Statistical post-test analysis and diagnostics improves the consistency, reliability, and accuracy of the diagnosed faults that will be presented as output from the test cell system. The statistical confidence bounds and fault classification techniques described herein will have significant impact on the detection of faults with increased confidence.
5. Spectral vibration plots taken over a wide range of engine operating conditions are easily distinguished so that only significant diagnostic anomalies and features are highlighted. Significant research by Impact in diagnosing engine mechanical faults has shown that "waterfall" and "tracked-order" vibration spectral plots are necessary for detecting most fault conditions.
6. The modular system architecture can be generic and easily applied to a wide range of engines and applications through the addition of relevant probabilistic knowledge databases including the risk assessment analysis results.
7. Operationally, the new capabilities will enable maintainers at both the base and depot level to diagnose engine faults either before engine tear down, or after re-build, thereby in both cases maximizing the chance of correctly diagnosing the

fault first time and thus avoiding re-work and increased down-time. The savings in man-hours and aircraft down time would be considerable.

Although this list of benefits is significant, it is anticipated that all of these improvements can be made with the specified hardware and software technologies described herein.

2.HARDWARE UPGRADE FOR THE F404 ENGINE TEST CELL

The upgrade of engine test cell hardware with the goal of supporting a modular and comprehensive engine diagnostic capability that provides integrated mechanical and performance based troubleshooting and diagnostics is currently being performed in Jacksonville. Engine data currently sensed and recorded during test cell operations must be analyzed in both a continuous real-time and post-test mode. The real-time diagnostics will continuously check for instrumentation faults, detect vibration and performance anomalies, classify module specific engine faults, and “virtually” sense non-measured parameters. The post-test diagnostics will examine the entire engine test data set to produce a more complete diagnostic assessment for both vibration and performance faults. In particular, statistical methods will be implemented to assess the confidence levels associated with particular fault scenarios classified by different fault detection methods. This hardware implementation will involve the following major considerations:

1. Provide an architecture that is “open” in the sense that it can be integrated with USAF, US Navy, and commercial test cell systems.
2. Provide a hardware configuration that allows for significant growth in both the diagnostic modules and engine databases.
3. Provide an overall test cell operating system (O/S) and associated application language to maximize portability across different test cell hardware platforms.

In the upgraded hardware configuration, engine testing is controlled by a system that consists of a Host Computer running a custom Gas Turbine Engine Control Software (GTECS) package developed by Sytronics, a VXI based Data Acquisition System, an Endevco TFAS vibration subsystem, and a PCT model PS5 Throttle Controller. An internal LAN connects the systems together and links it with a Software Development Station. A diagnostic computer is integrated into the test cell system via an ethernet link.

The host computer specified for the F404 test cell upgrade is an Intel Pentium III based machine running the Linux operating system with GTECS application software. Operators interface with the system through two 17”

touch-screen X-terminals for control and two 21” X-terminals for data display. The Host Computer communicates with the throttle controller and the Test Cell Calibration system over RS-232 links and acquires data via Ethernet from the Data Acquisition System. Figure 1 shows the operator interface for the F404 Test Cell Upgrade.



Figure 1 – F404 Hardware Upgrade Operator Computer

The data acquisition system is VXI based with a National Instruments Pentium III 450 MHz Windows 98 based Slot 0 controller, two HP E1413C A/D cards, an HP E1418A D/A card, an HP CENC-TAC8 Frequency Input card, two DDC 37001 Synchro/Resolver cards, two HP E1458A Digital I/O cards and a Systran DTI-GOLD/S MIL-STD-1553 Bus card. The Slot 0 Controller manages the data acquisition and sends all data to the host computer, via ethernet, at a rate of 50 updates per second. The Slot 0 controller also communicates with the Endevco TFAS Vibration Subsystem via an IEEE-488 communications link.

The diagnostic computer will be a stand-alone system running the engine diagnostics software. Data from the host computers will be transferred to the diagnostic computer via the Ethernet link during each engine run, or at the command of the test cell operator. The operator/engineer can also run the diagnostics on the engine data in a post-test mode for particular tests.

The hardware and associated data collection mechanism must compliment the diagnostic software technologies being implemented. The specifications and enhanced capabilities have been specifically identified with these goals in mind. For the main gas path performance measurements, low rate data acquisition (1-10 Hz) will be set by the GTECS computer system and stored as part of the test results file. For vibration measurements, higher rate data acquisition will be implemented and is discussed below. The GTECS system formats the appropriate data

and sends it to the diagnostic computer during each engine run and in real-time during the test.

There is a wide range of available measurements taken from an engine during test cell operation. Various pressure and temperature readings at different points within the gas path are required for performance assessment. Measurements at the engine inlet interface (station 1), HP compressor inlet (station 25), HP compressor discharge (station 3), LP turbine inlet (station 42), and exhaust (stations 6-9) are being utilized in this program, but are not always typical from engine/test cell to engine/test cell. Bleed flows, fuel flow, rotor speeds, airflows and other performance related engine conditions are also measured.

In a parallel but separate process, high rate vibration data (10KHz) is also gathered by an Endevco TFAS Vibration Subsystem consisting of two, 4 channel Tracking Filters

cards, eight Vibration Amplifier cards, and a processor card. The TFAS receives configuration commands from and sends FFT data to the VXI Data Acquisition system via IEEE-488. The vibration amplifier cards receive input from velocity coil vibration pickups and provide DC outputs for Amplitude Frequency and Phase. These DC outputs are read by the VXI's A/D inputs. The TFAS also provides broadband outputs that can be used for high-speed vibration data.

The VXI's Slot 0 Controller software was modified to acquire vibration data from the TFAS broadband analog output channels at a rate of 10 KHz, as required, and store this data in a file on it's local hard disk. Upon command from the test cell Host Computer, the VXI controller will transfer this data to the Host Computer for formatting and transfer to the Diagnostic Computer for use by the Diagnostics program.

Table 1 –Vibration Measurement Upgrade Requirements

Vibration Channels	2 (minimum); 4 (desired); 8 (maximum)
Type	Differential, ac coupled (5 Hz)
Voltage Range	0 to ± 10 V peak
Resolution	12-bit A/D (± 10 V = 4096 bits) minimum
Accuracy	Better than 1%
Sampling Rate	Minimum of 2500 Hz. - Preferred at 10 kHz
FFT lines	Minimum of 2048 – Preferred at 4096 or higher
Frequency Range	1 Hz to 1 kHz (frequency resolution < 2.5 Hz.)
Input Impedance	1 M Ohms
Vibration Sensors	Uses existing engine pickups; also accept ground test cell pickups.
<u>SPEED SIGNALS</u>	
Channels	N1 (standard); N2/N3 (optional)
Type	Single-ended, ac coupled (5 Hz)
Speed Signal	Discrete 1/rev or automatically locates imbedded 1/rev reference on any N1
Sensor Type	Uses existing engine N1 signal from magnetic sensors or tach-generator. Also accepts optical tach, strobe, etc. with no adjustment.
Voltage Range	50 mV to 100 V peak, autoranging
Frequency Range	1 Hz to 15kHz
Accuracy	Better than 1%
Input Impedance	100 K Ohms

3. SENSOR VALIDATION UPGRADE FOR F404 TEST CELL

For the hardware upgrade discussed above, a 10 Hz data acquisition rate was specified for the gas path performance parameters being implemented. The F404 temperature, pressure, flow, and speed measurements will be assessed by both a sensor validation module to detect sensor failures, and by a performance diagnostics module to detect performance faults. Data has already been collected on 14 F404 engines using the new test cell instrumentation hardware previously discussed.

Due to the fact that sensor malfunctions have traditionally played a major role in contributing to test cell problems and ineffectiveness, a principle goal of this software upgrade was to develop the capability to isolate and, in some cases, diagnose sensor faults. The approach that was developed utilizes generic signal processing techniques such as digital filtering and cross correlation coupled with intelligent classifiers including a fuzzy logic rulebase and neural networks to diagnose malfunctioning sensors (Roemer, et. al. 2001). To focus the effort, test cell operators at the Jacksonville NAS were interviewed to identify the most common sensor malfunctions on the F404-F1D2 engine. Table 2 lists the most common sensor malfunctions reported by the test cell operators. Historically, the test cell operators discarded data containing sensor malfunctions that is useful for the calibration and validation of the sensor diagnostic algorithms. Data exhibiting sensor malfunctions is now saved for future use.

Table 2 – Table 2 - Common Sensor Malfunctions

OEM accelerometer harness
Test cell accelerometers
Compressor guide vane sensor
Fan guide vane sensor
Engine temperature probes (CIT)
Engine pressure probes (PT5)
EGT thermocouples
Wiring harness connections

Custom data fusion tools were utilized to implement the sensor validation module illustrated in Figure 3 (Roemer, et. al. 2001). In this process, the initial stage of the sensor validation is performed on the raw data received from the entire sensor array by: first, screening the signals received from each sensor to insure their magnitudes lie within an expected range of operation, and second, applying generic signal processing techniques that correlate various signals in the incoming sensor array. These methods are used in conjunction with two artificial intelligence methods, which make up the second tier. In the final tier the results obtained from the signal processing evaluations must then be compiled and an evaluation made concerning the

validity of the signals being received. The sensor validation fusion provides the processing framework within which this evaluation takes place. The output of the sensor validation fusion process not only includes a determination concerning the validity of the signal received but also, in some cases, a diagnosis of the type of sensor fault detected. The capability of such diagnoses includes sensor cross talk, noise, spiking, saturation, and loss of signal.

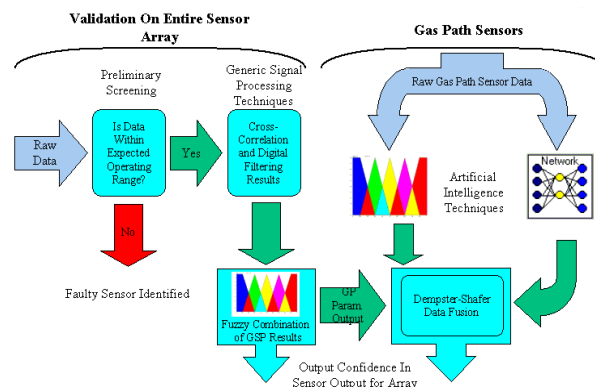


Figure 2 – Data Fusion Architecture for F404 Sensor Validation

The sensor validation implementation employed the Dempster-Shafer algorithm (Leferve, et. al., 1999 and Brooks '98). Briefly, in the Dempster-Shafer approach, uncertainty in conditional probabilities are considered and the methodology hinges on the construction of a set, called the frame of discernment, which contains every possible hypothesis. Every hypothesis has a belief denoted by a mass probability (m). Beliefs are combined in the following manner.

$$Belief(H_n) = \frac{\sum_{A \cap B = H_n} m_i(A) \cdot m_j(B)}{1 - \sum_{A \cap B = 0} m_i(A) \cdot m_j(B)} \quad (1)$$

Where A and B are two pieces of information with a probability and uncertainty. For the sensor validation problem, outputs from collaborating anomaly detection algorithms are fused together to provide increased sensor fault detection. Figure 4 illustrates the results obtained from applying the Dempster-Shafer fusion method to the regions of the data set identified as pseudo steady state. Here, the input to the fusion algorithm is the output from the two independent artificial intelligence modules utilized in the sensor validation schema applied to the engine data set. Both methods are assigned an equal uncertainty of 0.2 or ± 0.1 . The Dempster-Shafer method requires symmetric uncertainties and also that the combined values of the confidence \pm the uncertainty remain in the interval [0 1].

The results of the sensor validation fusion routine illustrates the benefit of the Dempster-Shafer method in fusing collaborating diagnostic output data. Two or more independent sources of data, reaching similar conclusions with similar uncertainties will reach a conclusion with greater confidence and decreased uncertainty than any single input. Here, one input comes from the fuzzy logic algorithm, the other from the neural network module, both give a high ($> 80\% \pm 10\%$) confidence value in the turbine inlet temperature sensor over much of the duration of the engine test run. The confidence level resulting from the fusion process is over 96% with an uncertainty of $\pm 2.1\%$. Figure 4 depicts the drops in confidence levels, which correspond to the spikes present in the TIT and PT54 sensor outputs. Figure 4 also illustrates a decrease in the confidence level of the fuzzy logic results in the region around the 1300th data point. This corresponds to the region of the trough shown in the N1 sensor. The two remaining confidence drops shown in the turbine inlet temperature plots are the result of slow transients resulting from the decelerations which had previously taken place. Notice the Dempster-Shafer combination still shows a confidence level above 80 % for these two regions.

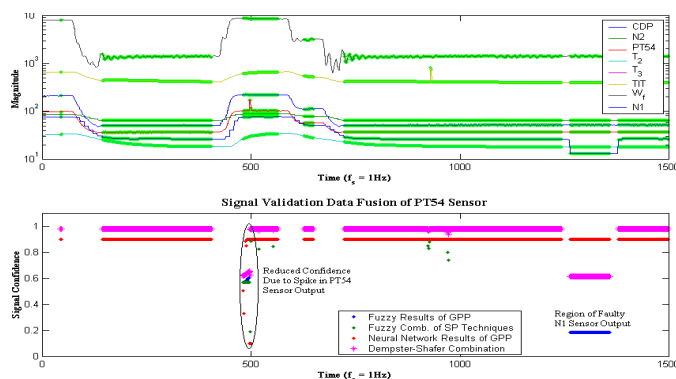


Figure 3 – Data Fusion Results from Test Cell Validation

4. PERFORMANCE DIAGNOSTICS UPGRADE FOR THE F404 TEST CELL

As an additional goal of the test cell upgrade, it was determined that improved engine performance assessments were needed as an integrated tool within the test cell software. To this end, a model-based performance fault detection and diagnostic module is being developed and implemented. The performance diagnostic approach relies on pattern recognition algorithms to compare the current performance parameters with known performance faults based on the F404 performance models.

As a critical input to the model-based analysis, probabilistic engine signature curves are developed for assessing the difference between an engines performance as compared to a “gold” or “correlator” engine or itself (from a previous test run). Standard-day corrected

engine instrumentation data must be utilized. Based on individual engine test runs for the F404, the statistical distributions associated with a specific test point(s) (i.e. Military Power) are developed that allow for performance shift detection to within a very small percentage for a specific engine.

After a rigorous filtering and data conditioning process, the algorithm performs a statistical multi-variant regression on key engine performance parameters. Standard statistical tests are automatically performed on the coefficients of 1st thru 6th order polynomials to determine their statistical significance, ensuring the best possible non-linear fit. This routine is well proven and further defined in Applied Linear Statistical Models by Neter, et al. The engine signature curves defined by this non-linear regression serve as the basis for assessing engine performance. The end results are signature curves similar to those shown in Figure 5.

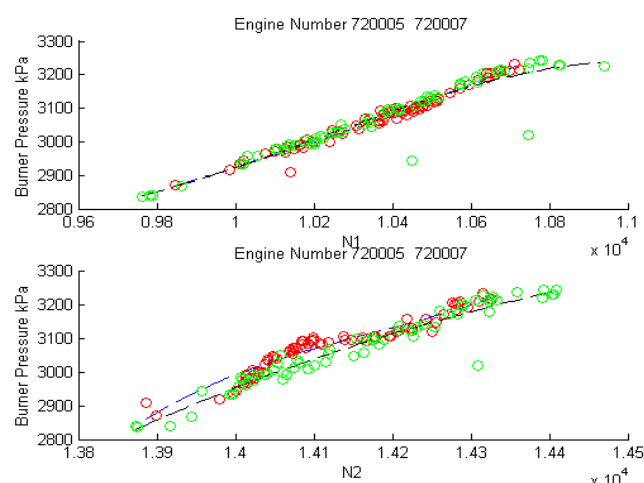


Figure 4 – Engine Signature Curve Analysis for Spool Speeds and P_3

The curves shown in Figure 5 depict the regression analysis performed for two different engine serial numbers (ESN's). By visual analysis alone, it is evident that the curves are statistically different. However, a more rigorous statistical approach has been implemented to determine if a statistically significant shift in the mean line function has occurred. The probability density functions at a particular speed are shown in Figure 6 and indicate the hypothesis of a shift in mean is supported by the t-test statistic used for 2 independent samples where the means are known but standard deviations are unknown but approximately equal (Montgomery '97):

$$\Delta = (\bar{X}_1 - \bar{X}_2) \pm t_\alpha S_p \sqrt{\frac{1}{n_1} + \frac{1}{n_2}} \quad (2)$$

$$\text{where; } S_p^2 = \frac{\sum (X_{1i} - \bar{X}_1)^2 + \sum (X_{2i} - \bar{X}_2)^2}{(n_1 - 1) + (n_2 - 1)}$$

Where:

- X_{1i} : i^{th} term of X_1
 \bar{X}_1 : mean of X_1
 X_{2i} : i^{th} term of X_2
 \bar{X}_2 : mean of X_2
 n_1 : sample size of data set 1
 n_2 : sample size of data set 2
 t_α : t statistic for α level of confidence
 Δ : interval over which hypothesis H_0 holds

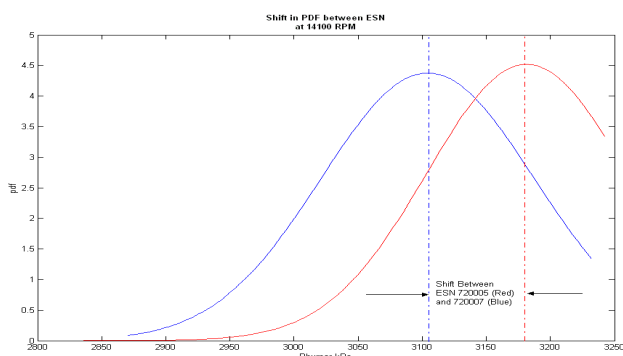


Figure 5 – Detecting a Shift in PDFs at a Given N2

Given the fact the actual performance faults only manifest themselves as minor shifts in the signature curves, this difference between two engine serial numbers warrants the need for each engine having a unique set of signature curves assigned to it. Although only one engine parameter is shown here, a complete set of engine signature curves and associated PDF's (as a function of speed) need to be developed to assess the performance of the engine. The detected shifts in key performance parameters are important in insuring accurate diagnosis of performance faults and robust engine-to-engine comparisons. The test cell performance diagnostic algorithm relies on gauging the proximity of the current system deviations to known performance faults based on the engine performance model. The model can either be the Official Equipment Manufacturer (OEM) developed DEC model or a steady-state model with the ability to assess off-design conditions. The important point is that the expected error patterns used to classify the engine performance faults is based on this model. An example of a steady state performance model that can be utilized for assessing off-design conditions of the engine is described briefly in the following section

Steady-State Performance Model

The development of a generic engine performance model that (without the need for compressor/turbine maps) has the ability to be adapted based on geometric conditions and can be “tuned” based on data gathered in the test cell. Also, in order to remain as generic as possible, a modular architecture is used for the modeling environment and a particular engine model can be generated from a simple

initialization file. A small library of generic components has been developed which contains constitutive equations and input/output blocks from adjoining components and from an initialization file. These generic engine component blocks can be combined to form many different engine configurations. Figure 7 shows a high level view of the Simulink model for the engine with the various engine modules/components clearly visible.

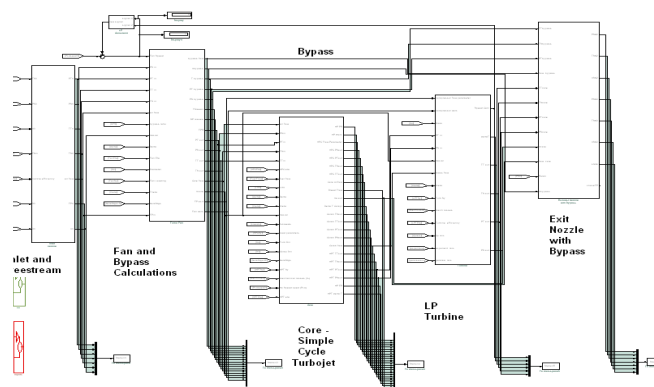


Figure 6 – Engine Performance Model Block Diagram

The initialization file is used to configure the steady state (S.S.) model to a particular engine type. Information in this file includes basic geometry such as inlet diameter, bypass ratio, number of compressor stages, etc. and other information such as Lower Fuel Heating Value and initial seed values for efficiencies and shaft speeds. Aside from the initialization file, the sensed inputs to the thermodynamic model are ambient temperature and pressure, inlet Mach number, PLA and fuel flow. Alternately, if the total pressure in the bellmouth is available, the Mach number is not required.

The modeling operation starts by “seeding” an initial condition for compressor/fan module. That speed is then utilized to calculate the power requirements of the compressor/fan. As soon as the power requirements are known, they are “matched” to their respective turbine where the turbine speed for that power is calculated from first principles. The process then iterates to balance the energy and angular momentum between the two machines. An example of component matching of a generic fan/turbine is briefly described next:

The change in total temperature across the turbine (ΔT_{T1}) is related to the turbine efficiency and the total pressure ratio (P_{T7}/P_{T8}) by:

$$\Delta T_{T1} = \eta_{T1} T_{T7} \left[1 - \left(\frac{1}{P_{T7}/P_{T8}} \right)^{\frac{\gamma-1}{\gamma}} \right] \quad (3)$$

The power output of the turbine (T1) must be equal to the power delivered to the flow by the fan, less the

mechanical losses ($\eta_m = 0.98$). Therefore, the relationship between the fan and the turbine (T1) is given by:

$$\left(\frac{mfr_{act}}{BPR + 1} + mfr_{fuel} \right) c_{pg} \Delta T_{TT1} = \frac{1}{\eta_m} mfr_{act} c_{pa} \Delta T_{Tf} \quad (4)$$

Where: BPR = Bypass ratio
 Mfr = mass flow rate actual
 ΔT_T = Total Temp change

By combining the above equations, the following relationship is obtained and used to match the two machines on the basis of energy conservation (Bathie, '96).

$$\left(\frac{P_{T1}^{\frac{\gamma-1}{\gamma}}}{P_{T1}} - 1 \right) = \eta_m \eta_f \eta_{T1} \left(\frac{1}{BPR + 1} + \frac{mfr_{fuel}}{mfr_{act}} \right) \frac{c_{pg}}{c_{pa}} \frac{T_{T1}}{T_{T1}} \left[1 - \left(\frac{P_{T7}}{P_{T8}} \right)^{\frac{\gamma-1}{\gamma}} \right] \quad (5)$$

Conservation of mass, unlike energy and angular momentum, is not confined to the compressor-turbine set to be balanced. For two spool machines, the compatibility between spools is met via aerodynamic coupling. Therefore the flow cannot exceed that which is allowed by a choked nozzle or turbine stators even though the overall pressure ratio can be increased.

In order to examine the accuracy of the thermodynamic model (initialized to a particular engine configuration), it needs to be validated with respect to engine test cell data. In this case the engine model was compared with 21 different engines at various operating conditions obtained from various test cell facilities. It should be noted that at the time these results were generated, the model did not yet fully account for bleeds, or variable geometry (IGV, VSV, or the exhaust nozzle). Figure 8 shows a comparison of T45 between the model and the 21 engines. For this feature the model appeared to be generally within 1% error, good enough to use for diagnostic purposes.

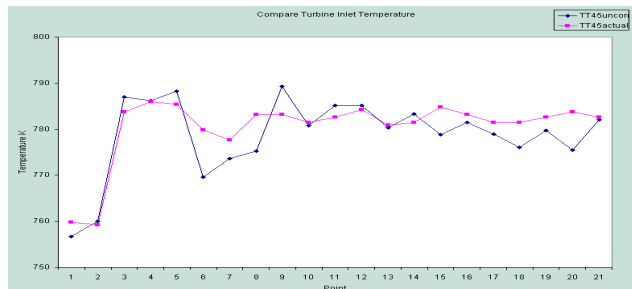


Figure 7 – Measurement vs. Model Comparison of T45

The final step in the performance diagnostic process involves mapping the measured parameter deviations to the modeled engine faults. Hence, this performance model or alternatively an OEM DEC model is used to generate performance error patterns or diagnostic scalars

used for fault isolation. As illustrated in Figure 9, the diagnostic scalars are simply the differences between the model estimate and the measured values of key performance parameters shifts (Wf,N2,T45,P25,T25,T3,P3) at referred conditions. When these error patterns are generated, the next step is to consider the influence of root cause performance faults on the key performance parameters. A set of root cause performance faults for the F404 are: Fan Eff., LPC Eff., HPC Eff., HPT Eff., LPT Eff., 2.5 Bleed, 2.9 Bleed, Discharge Area, and Stator vane misrigging.

Different severities of these faults will create different performance parameter error patterns that must be contained in the “Engine Specific Baseline Characteristics” database. Although actual engine faults would be ideal for producing the fault error patterns, simulating them with the engine model a priori is the only real practical approach in some cases.

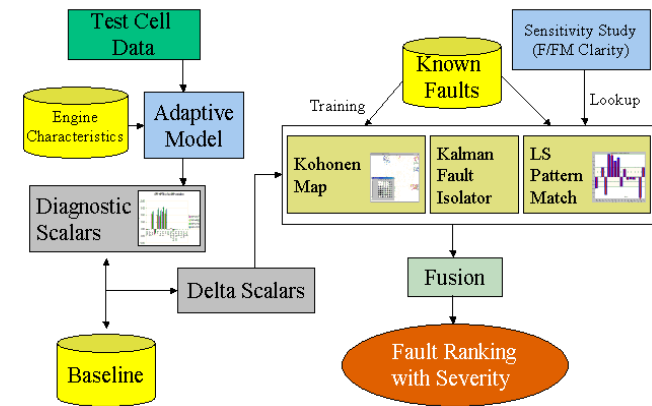


Figure 8 – Performance Diagnostic Process

With the error pattern calculated, the database of known faults must be autonomously compared with the current delta scalar pattern to enable real-time performance assessments. In reality, the data-driven error pattern will not exactly match any of the calculated (ideal) error patterns so the most likely root causes must be determined. In this program, two unique methods are utilized for performing this task. They include a least squares pattern match algorithm and a Kohonen Map/Neural Network classification technique. These error pattern classification techniques have already been shown to be capable of identifying degraded performance in propulsion systems (Roemer, et. al. 1999 and Volponi, et. al. 2000). Modeling and measurement uncertainty is accounted for with this technique utilizing the distributions on the current parameter shifts and model-based fault conditions.

5. TROUBLESHOOTING GUIDE UPGRADE FOR THE F404 TEST CELL

Engine test cell troubleshooting involves identification of the most likely maintenance actions by evaluating the results of a logical path of observations and measurements. Traditionally, troubleshooting is initially performed with a manual and then develops into an intuitive process as the maintenance person gains experience. A troubleshooting approach that combines the original equipment manufacturer's (OEM's) manual, with a-priori knowledge of experienced technicians is under development to optimize the troubleshooting path. By capturing the expertise of key test cell personnel, the troubleshooting software will also help stem the loss of troubleshooting capability due to staff turnover. Bayesian Belief networks will combine information from the OEM's troubleshooting manual and a-priori knowledge with diagnostic information supplied by the user to efficiently identify the required maintenance action.

Experienced test cell operators at the Jacksonville NAS were interviewed to solicit their troubleshooting experience in terms of identifying common faults and associated diagnostic procedures for the F404 engine. Technicians were asked to estimate the probability of occurrence for each fault, and where possible, document failure rates with data from maintenance logs. The interviews also revealed a strong desire among the test cell operators for more complete and relevant troubleshooting documentation than that provided by the OEM. While the test cell operators are satisfied with the wiring diagrams in the OEM's troubleshooting guide, they cited examples of common malfunctions that are not covered by the existing troubleshooting guide.

expert knowledge level to modify the underlying Bayesian belief networks (Figure 10) as the troubleshooting knowledge base grows to include new or rare failure modes and associated diagnostic procedures. A software interface has been designed for the automated troubleshooting guide. Figure 11 illustrates the functionality of the main screen. The troubleshooting process begins in the upper portion of the screen with the selection of a malfunction. A dialog box displays the known malfunctions in an easy-to-use expandable tree structure as shown in Figure 12.

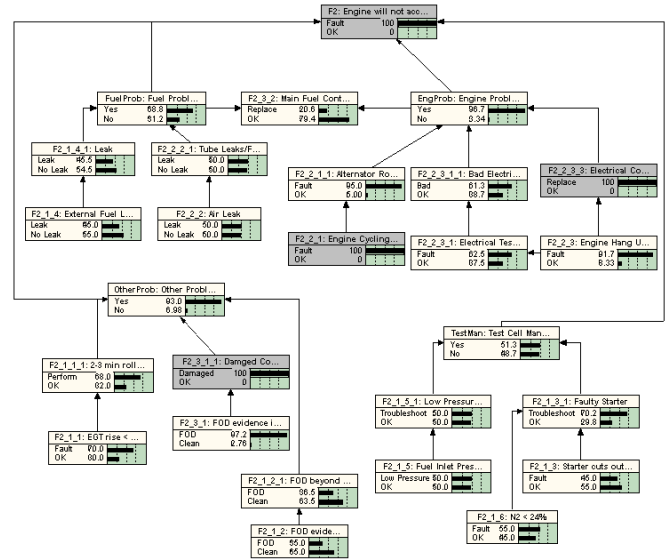


Figure 10 – Example of a Bayesian Belief Network for a Hung Start

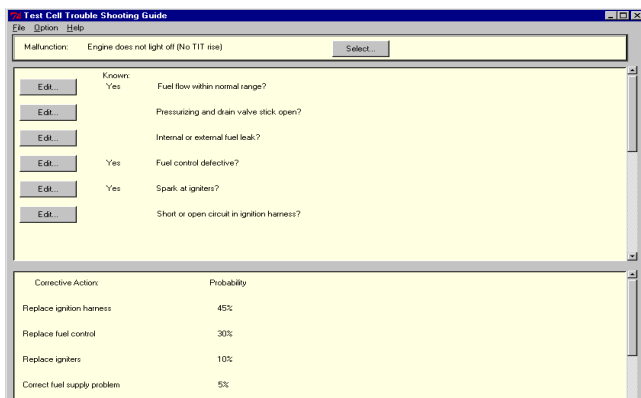


Figure 9 – Test Cell Troubleshooting Guide (TCTG) main screen

In response to the need for a more complete and relevant troubleshooting guide, the upgraded software will allow users with administrative privileges to add new malfunctions and diagnostic procedures. This integral feature of this software module will allow users with an

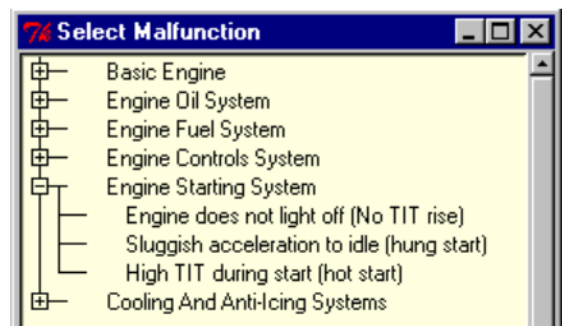


Figure 11 – Troubleshooting Guide Malfunction Selection

Once a malfunction has been selected, a prioritized list of troubleshooting measures is presented in the middle portion of the main screen. The questions that, based on a-priori knowledge of failure rates, are most likely to isolate the fault appear at the top of the list so as to direct users down the most efficient troubleshooting path. Questions may be answered using Boolean expressions such as true/false or with degrees of certainty as shown in Figure 12. In situations where the evidence requested is not available, users can obtain the best possible diagnosis

based on the available information and the a-priori probabilities that serve as default values for each piece of evidence.

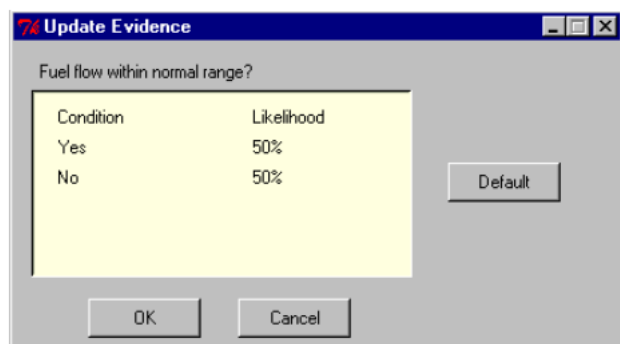


Figure 12 – Troubleshooting Guide Evidence

6. CONCLUSIONS

This paper has introduced several concepts that need to be considered when examining the decision for upgrading military engine test cell capabilities. From a hardware upgrade standpoint, a suitable architecture with associated data capture rates was presented that allows for easy integration of newly developed health management modules. In terms of improved engine fault detection and isolation capabilities, various approaches for automated sensor validation, performance diagnostics and troubleshooting were described. Specifically, the techniques were recently developed and implemented for the TF-39 engine and are now being implemented at the NAS in Jacksonville for the F404 engine test cells. We expect the capabilities of this upgraded F404 test cell to satisfy system requirements of reduced support costs and improved engine testing and accountability. Additional data continues to be collected under this test cell upgrade effort and determination of the cost/benefits of this program is underway.

REFERENCES

- [1] Agosta, J. M., and Weiss, J. W., "Active Fusion for Diagnosis Guided by Mutual Information Measures", Proceeding of the 2nd International Conference on Information Fusion, July 6-8, 1999
- [2] Brooks, R. R., and Iyengar, S. S, Multi-Sensor Fusion, Copyright 1998 by Prentice Hall, Inc., Upper Saddle River, New Jersey 07458
- [3] Neter, John, Kutner, Michael H., Nachtsheim, Christopher J., and Wasserman, William, Applied Linear Statistical Models, IRWIN, Chicago, 1996.
- [4] Roemer, M. J., Kacprzyński, G. J., Orsagh, R. F.,

"Strategies for Prognostics and Health Management", IEEE Aerospace Conference, Big Sky, Montana, 2001.

- [5] Hall, D., and Llinas, J., "An Introduction to Multisensor Data Fusion", Proceedings of the IEEE, January 1997.
- [6] Leferve, E., and Colot, O., "A classification method based on the Dempster-Shafer's theory and information criteria" Proceeding of the 2nd International Conference on Information Fusion, July 6-8, 1999.
- [7] Roemer, M. J., Kacprzyński, G. J., Schoeller, M., "Advanced Test Cell Diagnostics for Gas Turbine Engines", IEEE Aerospace Conference, Big Sky, Montana, 2001.
- [8] Orsagh R.F., Roemer M.J., et al "Development of Metrics for Mechanical Diagnostic Technique Qualification and Validation", COMADEM Conference, Houston TX, December 2000.
- [9] Roemer, M. J. and Kacprzyński, G.J., "Advanced Diagnostics and Prognostics for Gas Turbine Engine Risk Assessment," Paper 2000-GT-30, ASME and IGTI Turbo Expo 2000, Munich, Germany, May 2000.
- [10] Gladney, Ed. "NASA Launches an Automated Data Acquisition System", Sensors, September 1998.
- [11] Roemer, M. J., and Ghiocel, D. M., "A Probabilistic Approach to the Diagnosis of Gas Turbine Engine Faults" Paper 99-GT-363, ASME and IGTI Turbo Expo 1999, Indianapolis, Indiana, June 1999.
- [12] Roemer, M. J., and Atkinson, B., "Real-Time Engine Health Monitoring and Diagnostics for Gas Turbine Engines," Paper 97-GT-30, ASME and IGTI Turbo Expo 1997, Orlando, Florida, June 1997.
- [13] Byington, C.S., Kozlowski, J.D., "Transitional Data for Estimation of Gearbox Remaining Life", Proceedings of the 51st Meeting of the MFPT, April 1997
- [14] Bathie, W., Fundamentals of Gas Turbines, John Wiley & Sons, 2nd Ed.
- [15] Volponi, A., et. al., "The Use of Kalman Filter and Neural Network Methodologies in Gas Turbine Performance Diagnostics: A Comparative Study" IGTI, 2000
- [16] Montgomery, D., Design and Analysis of Experiments, John Wiley & Sons, 1997